Supporting Information:

Enzymatic ring opening of an iron corrole by plant-type heme oxygenases: Unexpected substrate and protein selectivities

Björn Gisk, Frédérique Brégier, Robin A. Krüger, Martin Bröring, and Nicole Frankenberg-Dinkel

Material and Methods

Expression and purification of recombinant heme oxygenases

Details on expression and purification of the various heme oxygenases have been described earlier (*1, 2*). In brief, *Arabidopsis thaliana* HO1 (HY1), *Synechocystis* sp. PCC6803 HO-1, BphO and PigA of *Pseudomonas aeruginosa* were recombinantely produced as N-terminal glutathione-S-transferase (GST)-fusions in *Escherichia coli* while *Arabidopsis thaliana* HO3 and HO4 both contained a C-terminal hexa-histidine tag. All plant HOs lacked the predicted chloroplast transit peptide sequence. Truncated human HO1 (*3*) was expressed in *E. coli* and subjected to a 60 % $(NH_4)_2SO_4$ cut, dialyzed against reaction buffer and used as an enriched protein fraction similar to a method described in (*4*).
All proteins were dialyzed against reaction buffer (100 mM potassium phosphate, pH 7.2) prior touse.

Analytical size-exclusionchromatography

Analytical size-exclusion chromatography was employed to investigate the complex formation between the iron corroles of all five heme oxygenases. A Superdex^{TM} 75 10/300 GL column (GE Healthcare) equilibrated with 100 mM potassium phosphate, pH 7.2, at a flow rate of 0.5 mL/min, was used to analyze iron corrole:heme oxygenase complexes (1:1). During the run the absorbance at 280 nm and 398 nm / 535 nm using a UV-900 detector of an *AEKTA-Explorer* system (GE Healthcare) was detected.

Heme oxygenase assay

Iron corrole isomers were dissolved in DMSO and incubated with equimolar amounts of each HO for 10 minutes in reaction buffer (100 mM potassium phosphate, pH 7.2). Spectral changes were monitored using an *Agilent Technologies 8453* UV-visible Spectroscopy system. For catalytic turnover, the assay contained 10 µM HO, 20 µM iron corrole, 0.15 mg/mL bovine serum albumin, 4.6 µM ferredoxin (spinach), 0.025 unit/mL spinach ferredoxin-$NADP^+$ oxidoreductase and 10 µM catalase from *Aspergillus niger* in 100 mM potassium phosphate buffer (pH 7.2) in a total volume of 500 µl. The reaction was started by addition of an NADPH-regenerating system containing 6.5 mM glucose 6-phosphate, 0.82 mM $NADP^+$, and 1.1 unit/mL glucose-6-phosphate dehydrogenase. Spectral changes between 300 and 900 nm were monitored for 30 min at 25 ^oC using an *Agilent Technologies 8453* UV-visible Spectroscopy system. To detect the reaction product 5 mM of an iron chelator (e.g. Tiron) was added to the assay.

HPLC analyses

HO reaction products were acidified with tenfold 0.1% trifluoroacetic acid (TFA) and loaded onto a Waters (Milford, MA, USA) C18- Sep-Pak Light cartridge preconditioned as follows: 3 mL acetonitrile to wet the Sep-Pak, 3 mL MilliQ water, 3 mL 0.1% TFA, 3 ml 10% methanol in 0.1% TFA, 3 mL acetonitrile, 3 mL MilliQ water, 3 mL 10% methanol in TFA. After the sample was loaded onto the Sep-Pak, it was washed with 6 mL 0.1% TFA, and 6 mL 20% methanol / 80 % TFA (0.1%). The pyrroles were then eluted from the Sep-Pak using 1 mL of 100% acetonitrile. The eluate was dried using a Speed-Vac lyophilizer and

subsequently analyzed by HPLC. The dried sample was first dissolved in 10 µL DMSO and then diluted with 150 µL of the HPLC mobile phase. Following brief centrifugation (10.000 × g for 1 min) and filtration through a 0.45 µm polytetrafluoroethylene syringe filter, the pyrroles were analyzed by reversed phase chromatography using an *Agilent Technologies 1100* liquid chromatograph. The HPLC column used for all analyses was a 4.6 x 250 mm Phenomenex Ultracarb 5 µm ODS(20) analytical column with a 4.6 x 30 mm guard column of the same material. The mobile phase consisted of acetone, isopropanole, and 20 mM formic acid (33:33:33 by volume), and the flow rate was 0.6 mL/min. The eluate was monitored at 650 nm and 380 nm using an *Agilent Technologies 1100* series diode array detector. A standard (synthetic bilindione **3**) was analyzed the same way.

Material and instruments for the chemical compounds

Starting materials and reagents were obtained from commercial sources and used as received. All solvents were dried by standard procedures and stored under a blanket of nitrogen. ^{1}H NMR spectra were obtained with a *Bruker Avance 300* or a *Bruker DRX-400* spectrometer. Chemical shifts (δ) are given in ppm relative to residual protio solvent resonances. High resolution mass spectra (APCI, ESI) were recorded with an *IonSpec Ultima*, a *Finnigan LTQ FT*, or a *QStarPulsar i*. UV-Vis spectra were measured on a *Shimadzu UV-1601 PC* in concentrations of about 10^{-5} mol L^{-1}. CHN analyses were recorded on a *Elementar Vario EL*.

Synthesis of tetrapyrroles

[α-CH-Fe(cor)] **1**:

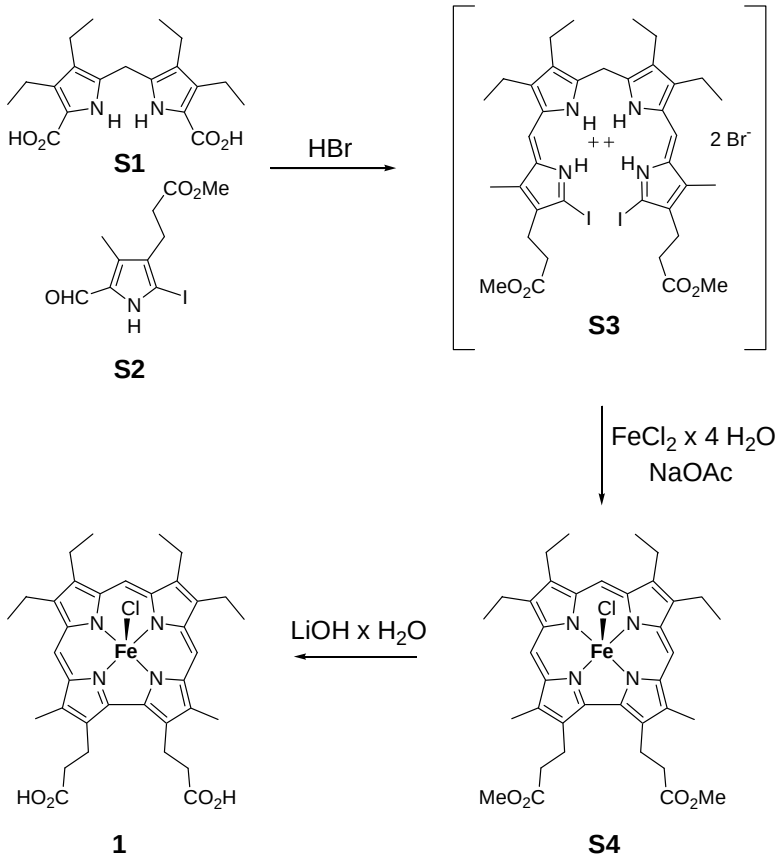

Dipyrrylmethane **S1** (*5*) (319.5 mg, 0.92 mmol) and iodopyrrole aldehyde **S2** (*6*) (591 mg, 1.84 mmol) were dissolved in hot ethanol (15 mL) and treated with hydrobromic acid (48% in water, 4 mL) at once. The solution was refluxed for three minutes and then cooled to 4°C to allow the product to crystallize over night as the bis(hydrobromide) **S3** (646.8 mg, 68%). This

material was dissolved in DMF (100 mL) under an atmosphere of nitrogen. $FeCl_2 \times 4\ H_2O$ (635 mg, 3.19 mmol) and NaOAc (262 mg, 3.19 mmol) were added, and the mixture was heated to 80°C for 7 hours. After cooling the solvent was removed in vacuo, the residue was redissolved in dichloromethane (50 mL) and washed twice with each, hydrochloric acid (1 mol/L, 100 mL) and water (100 mL). After drying with sodium sulfate all volatiles were removed in vacuo, and the residue was subjected to column chromatography on silica with dichloromethane/methanol (99:1). Recrystallization from dichloromethane/*n*-hexane yielded the iron corrole **S4** as a brown solid (207.1 mg, 47%). **Analytical data for S4:** $C_{37}H_{43}ClFeN_4O_4$ (699.06), calc. C: 63.57; H: 6.26; N: 7.91. Found C: 63.28; H: 6.27; N: 7.96. HRMS (ESI): calc. for $[C_{37}H_{44}FeN_4O_4]^+$ 664.2706; found: 664.2717; Δ = -1.1 mmu. ^{1}H NMR (400 MHz, CD_2Cl_2): δ = 192.08 (br. s, 1H), 178.98 (br. s, 2H), 32.14 (br. s, 2H), 27.62 (br. s, 2H), 19.13 (br. s, 2H), 16.71 (br. s, 2H), 15.82 (br. s, 6H), 3.93 (br. s, 2H), 3.66 (br. s, 6H), 1.67 (br. s, 2H), 1.35 (br. s, 6H), 0.08 (br. s, 4H), -0.14 (br. s, 6H). UV-Vis (CH_2Cl_2): λ_{max} (ε) = 295 (20600), 330 (30900), 371 (50100), 480 (8900), 524 (6600), 935 nm (530 M^{-1} cm^{-1}).

Saponification: Iron corrole **S4** (128.5 mg, 0.18 mmol) and $LiOH \times H_2O$ (101.3 mg, 2.43 mmol) were dissolved in THF (20 mL) and water (2 mL) and stirred at ambient temperature over night. Dichloromethane (20 mL) and hydrochloric acid (1 mol/L, 20 mL) were added, the layers were separated and the organic layer containing the title compound α-CH-Fe(cor) **1** was washed with water (50 mL). Drying with sodium sulfate and recrystallization from dichloromethane/*n*-hexane yielded a brown powder (86.4 mg, 70%). **Analytical data for 1:** HRMS (APCI): calc. for $[C_{35}H_{39}FeN_4O_4]^+$ 635.2315; found: 635.2336; Δ = -2.1 mmu. ^{1}H NMR (400 MHz, DMSO-d_6): δ = 194.2 (br. s, 1H), 179.3 (br. s, 2H), 30.9 (br. s, 2H), 28.0 (br. s, 2H), 21.0 (br. s, 2H), 19.1 (br. s, 6H), 18.2 (br. s, 2H), 4.1 (br. s, 2H), 2.5 (br. s, 6H), 1.5 (br. s, 2H), 1.0 (br. s, 2H), 0.7 (br. s, 6H), -6.2 (br. s, 2H). UV-Vis (KPi 50 mmol, pH 7.0): λ_{max} (ε) = 358 (35100), 520 sh (4400), 997 nm (2500 M^{-1} cm^{-1}).

[γ-CH-Fe(cor)] **2**:

This compound was prepared as reported in Ref. (*7*).

Bilindione **3**:

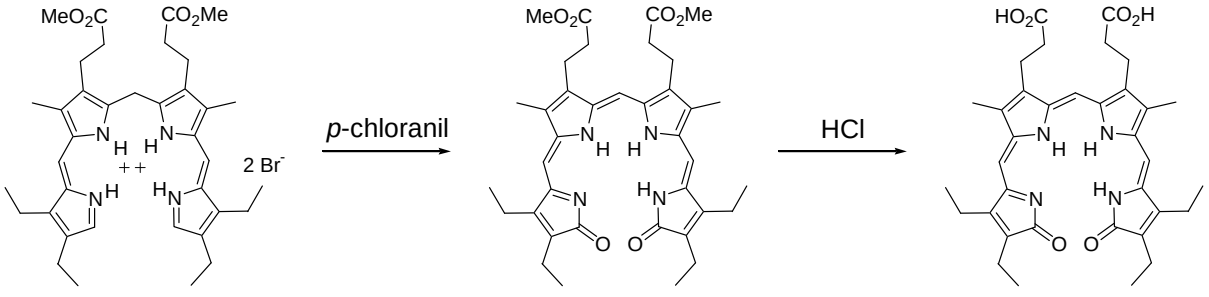

a,*c*-Biladiene as bis(hydrobromide) **S5** (*8*) (775 mg, 1.00 mmol) and *p*-chloranil (740 mg, 3 mmol) were dissolved in water-saturated chloroform and refluxed for 2 hours. After cooling the mixture was washed with water (3 × 20 mL), dried with sodium sulfate, and all volatiles were evaporated at reduced pressure. Chromatographic separation of the residue with dichloromethane on alumina and collection of the blue band yielded the bilindione dimethylester **S6** as a dark blue solid (290 mg, 45%). **Analytical data for S6:** HRMS (ESI): calc. for $[C_{37}H_{46}N_4O_6Na]^+$ 665.3310; found: 665.3318; Δ = 0.8 mmu. ^{1}H NMR (400 MHz, $CDCl_3$): δ = 8.22 (br. s, 3H), 6.73 (s, 1H), 5.90 (s, 2H), 3.67 (s, 6H), 2.92 (t, J = 7.6 Hz, 4H), 2.55 (t, J = 7.6 Hz, 4H), 2.51 (q, J = 7.6 Hz, 4H), 2.28 (q, J = 7.6 Hz, 4H), 2.08 (s, 6H), 1.24

(t, J = 7.6 Hz, 6H), 1.07 (t, J = 7.6 Hz, 6H). UV-Vis (MeOH): λ_{max} (ε) = 364 (50100), 640 nm (14600 M^{-1} cm^{-1}).

Saponification: Bilindione **S6** (12,8 mg, 20 μmol) and hydrochloric acid (conc., 2.5 mL) were mixed with glacial acetic acid (2.5 mL) and stirred at ambient temperature in the dark for 24 hours. Chloroform (20 mL) was added, the layers were separated and the organic layer containing the title bilindione **3** was carefully washed with aqueous sodium acetate (conc., 5 mL) and water (5 mL). Drying with sodium sulfate and recrystallization from dichloromethane/*n*-hexane yielded a blue powder (7.0 mg, 55%). **Analytical data for 3:** HRMS (ESI): calc. for $[C_{35}H_{42}N_4O_6Na]^+$ 637.2997; found: 637.2984; Δ = -1.3 mmu. ^{1}H NMR (300 MHz, D_2O): δ = 6.76 (s, 1H), 5.93 (s, 2H), 2.71 (t, J = 7 Hz, 4H), 2.43 (q, J = 7 Hz, 4H), 2.27 (t, J = 7 Hz, 4H), 2.11 (q, J = 7 Hz, 4H), 1.93 (s, 6H), 1.12 (t, J = 7 Hz, 6H), 0.94 (t, J = 7 Hz, 6H). UV-Vis (DMSO): λ_{max} (ε) = 374 (43300), 635 nm (14400 M^{-1} cm^{-1}).

References

1. Gisk, B., Yasui, Y., Kohchi, T., and Frankenberg-Dinkel, N. (2010) Characterization of the haem oxygenase protein family in *Arabidopsis thaliana* reveals a diversity of functions, *Biochem J 425*, 425-434.
2. Wegele, R., Tasler, R., Zeng, Y., Rivera, M., and Frankenberg-Dinkel, N. (2004) The heme oxygenase(s)-phytochrome system of *Pseudomonas aeruginosa*, *J Biol Chem 279*, 45791-45802.
3. Wilks, A., Black, S. M., Miller, W. L., and Ortiz de Montellano, P. R. (1995) Expression and characterization of truncated human heme oxygenase (hHO-1) and a fusion protein of hHO-1 with human cytochrome P450 reductase, *Biochemistry 34*, 4421-4427.
4. Wilks, A., and Ortiz de Montellano, P. R. (1993) Rat liver heme oxygenase. High level expression of a truncated soluble form and nature of the meso-hydroxylating species, *J Biol Chem 268*, 22357-22362.
5. Murakami, Y., Yamada, S., Matsuda, Y., and Sakata, K. (1978) Transition-metal Complexes of Pyrrole Pigments. XV. Coordination of Pyridine Bases to the Axial Sites of Cobalt Corroles, *Bull Chem Soc Jap 51*, 123-129.
6. Tu, B., Ghosh, B., and Lightner, D. A. (2003) A new class of linear tetrapyrroles: acetylenic 10,10a-didehydro-10a-homobilirubins, *J Org Chem 68*, 8950-8963.
7. Matsuo, T., Hayashi, A., Abe, M., Matsuda, T., Hisaeda, Y., and Hayashi, T. (2009) Meso-unsubstituted iron corrole in hemoproteins: remarkable differences in effects on peroxidase activities between myoglobin and horseradish peroxidase, *J Am Chem Soc 131*, 15124-15125.
8. Sengupta, D., and Robinson, B. C. (2002) Synthesis of chlorins possessing a fused naphthalene ring, *Tetrahedron 58*, 5497-5502.

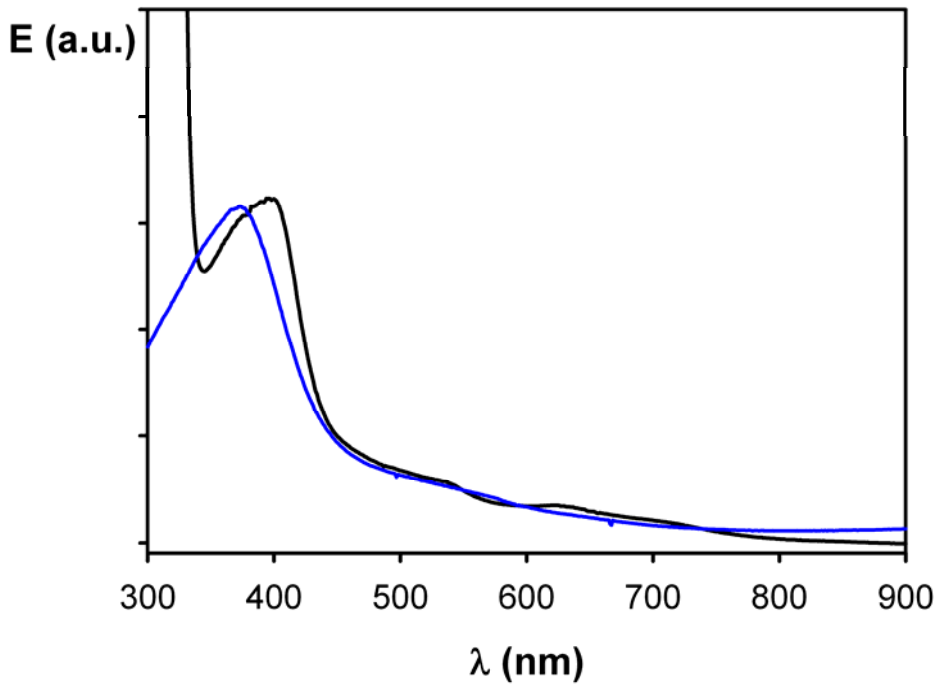

Figure S1. Absorption properties of iron corrole 2 (blue spectrum) in neutral aqueous solution (pH 7.2) and after addition of *P. aeruginosa* BphO (black spectrum). Interaction with BphO results in a shift of absorption from 376 nm to 400 nm and the occurrence of shoulders at ~540 nm and 620 nm.

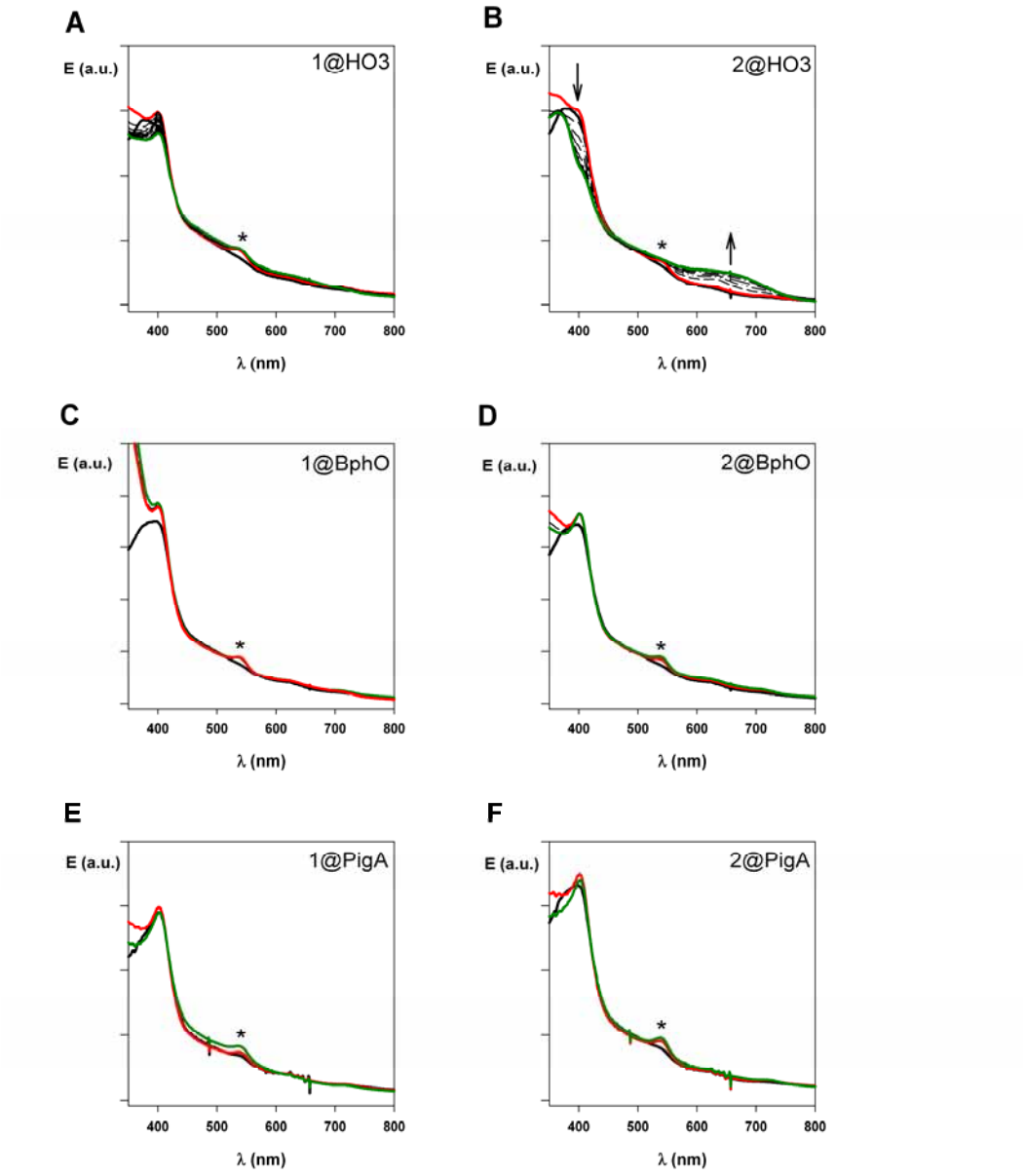

Figure S2: Spectroscopic characterization of the catalytic turnover of the regioisomeric iron corrole 1 and 2 in complex with the plant (HO3) and bacterial (BphO and PigA) HOs.

After formation of the iron corrole:HO complex (black spectrum), the reaction was started by the addition of an NADPH-regenerating system and time-dependent absorbance changes were monitored every minute over a period of 30 min. (**A**) HO3 reaction with iron corrole **1** containing an iron-chelator shows binding and reduction of the corrole but no conversion. (**C**) Iron corrole **1** in complex with BphO, (**E**) Iron corrole **1** in complex with PigA. Both HOs show binding and reduction but no conversion of iron corrole **1**. (**B**) HO3 reaction with iron corrole **2** containing an iron chelator first shows a reduced iron corrole species (red spectrum) which was converted to a product peak at 670 nm (green spectrum) and a decrease at ~400 nm. In contrast, binding and reduction but no conversion of iron corrole **2** in complex with BphO (**D**), and PigA (**F**) was observed. (*) indicates the electron changes of the center iron (535 nm) of the corrole and coordination through an axial imidazole-histidine within the HOs. The direction of spectral changes are indicated by arrows.

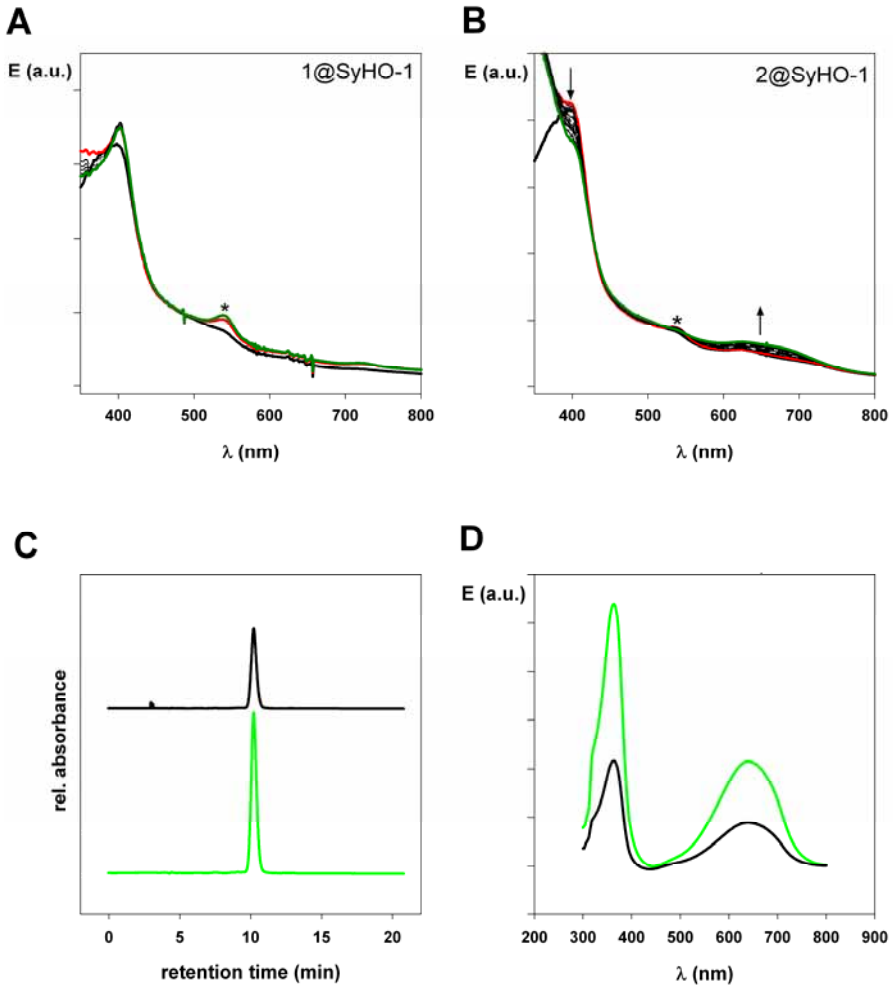

Figure S3: Spectroscopic characterization of the catalytic turnover of the regioisomeric iron corrole 1 and 2 in complex with the plant-type HO-1 from *Synechocystis* sp. PCC6803 (SyHO-1).

After formation of the iron corrole:HO complex (black spectrum), the reaction was started by the addition of an NADPH-regenerating system and time-dependent absorbance changes were monitored every minute over a period of 30 min. (**A**) SyHO-1 reaction with iron corrole **1** containing an iron-chelator shows binding and reduction of the corrole but no conversion. (**B**) SyHO-1 reaction with iron corrole **2** containing an iron chelator first shows a reduced iron corrole species (red spectrum) which was converted to a product peak at 670 nm (green spectrum) and a decrease at ~400 nm. (**C**) Comparison of HPLC (RP-C18 column developed with acetone, isopropanole, and 20 mM formic acid (33:33:33 by volume) and detected at 650 nm and (**D**) UV/vis characteristics (in acetone, isopropanole, and 20 mM formic acid (33:33:33 by volume)) of the product of the SyHO-1 catalyzed oxygenation of γ-CH-Fe(cor) **2** (black line), and the synthetic biliverdin analog **3** (green line). (*) indicates the electron changes of the center iron (535 nm) of the corrole and coordination through an axial imidazole-histidine within the HO. The direction of spectral changes are indicated by arrows.